ARCHIVES OF ELECTRICAL ENGINEERING VOL. 71(1), pp. 125–138 (2022)

DOI 10.24425/aee.2022.140201

# Calculations and measurements of torque and inductance of switched reluctance motors with laminated and composite magnetic cores

MAREK PRZYBYLSKI

*Łukasiewicz Research Network – Tele and Radio Research Institute*
*Poland*

*e-mail: marek.przybylski@itr.lukasiewicz.gov.pl*

(Received: 23.08.2021, revised: 07.10.2021)

**Abstract:** The performance of drives with switched reluctance motors (SRMs) depends on magnetic materials used in their construction which influence static parameters such as inductance and electromagnetic torque profiles. The paper deals with simulations of switched reluctance motors in the finite element method and their comparison with measurements. Two kinds of switched reluctance motors were analysed, the modified Emerson Electric motor with a laminated steel core and a prototype, the one with a magnetic core made of iron-based powder composite materials. In the first part of the research, magnetization curves of magnetic materials were measured for static and dynamic conditions with 50 Hz. Next, simulations and measurements of inductance and developed torque were compared and analysed. In the last part of the research, simulations of magnetic flux density in motors were conducted. As the result of the research, it occurred that the simulations and measurements are quite close and two kinds of motors exhibit similar performance.

**Key words:** electromagnetic torque measurements, inductance measurements, simulations, switched reluctance motors

## 1. Introduction

Nowadays, a lot of effort is put into the development of electric motors that have better performance than existing ones and have lower prices. Customers look for electric motors and drives that have high efficiency and do not need periodic maintenance such as the replacement of brushes. The main development is observed in brushless machines, especially permanent magnet synchronous motors, however, a switched reluctance motor (SRM) is a kind of electric motor

that is still under interest of their manufacturers and researchers. This type of motor has a lot of advantages such as e.g., a simple construction, only a stator has concentrated windings, lack of pricey permanent magnets, good efficiency, especially at high rotational speeds, high starting torque, and a broad range of rotational speed [1–4]. Nowadays, permanent magnets with rare earth elements such as samarium and neodymium are expensive, and their prices depend on their accessibility from China, their main supplier. That is why, the development of electric machines without permanent magnets [5,6], or with magnets with lower amount of rare earth elements [7] is still observed. Recently, we have not seen a new kind of hard magnetic material for the production of permanent magnets that could be applied in electric motors.

Soft magnetic materials that are applied in electric machines are mainly oriented and non-oriented electrical steels. They mainly consist of iron and have up to a few percent of silicone. In addition, silicone enhances resistivity of the material and causes lower eddy currents and loss of energy during changes of magnetic flux. Oriented electrical steel has easy direction of magnetization, they have magnetic anisotropy, and are mainly used in transformers. For electric motors, non-oriented electrical steel with isotropic magnetic properties in all magnetization directions is mainly used. By weight, electrical steels account for almost 95% of all applied soft magnetic materials, with a production of 7 million tonnes per year in 2010. It is almost 75% of the market value of soft magnetic materials with a value of nearly $6.3 billion per year [8]. It is based on very good magnetic properties and a low price of electrical steel. Electrical steel has also disadvantages, such as limited working frequency of magnetic flux or the necessity to create magnetic core from many laminations. Manufacturing of complicated magnetic cores from electrical steel sheets is sometimes very difficult to realize especially with the magnetic flux with 3-dimensional distribution such as claw pole or axial field machines. Looking for other cheap materials, the development of soft magnetic composite (SMC) materials should be mentioned.

Soft magnetic composite material is a relatively new material for the preparation of magnetic cores of electrical motors, generators, and other electromagnetic and electromechanical converters that work with changing magnetic flux. This type of material consists of compressed soft magnetic powder, mainly cheap iron with very good magnetic properties and dielectric material such e.g., epoxy or polyester resins, phosphates, oxides, or sulphates [9,10]. Each iron particle is surrounded by a dielectric and is subsequently pressed into a die shaped as the needed component. It could be e.g., a ring, cylinder or block. Pressing pressure depends on a kind of powder and is equal to about a few hundred of MPa. The average grain size of iron particles is equal to about a few hundred micrometres. Smaller sizes of magnetic particles are beneficial in decreasing eddy current loss however, it is difficult to press powder with very small particles and achieve a dense product. The obtained component is then cured in a furnace with temperature depending on the kind of dielectric material for approximately 0.5 to 2 hours. For resins it is about 200°C, for other materials it could be up to 600°C. Higher curing temperatures are needed, because they partially eliminate strains that occur in soft magnetic particles during curing, causing an increase of magnetic properties such as an increase of permeability and a decrease of iron loss.

In previous works a commercially available switched reluctance motor made by Emerson Electric company was analysed. This motor of the H55BMBJL-1820 type was produced with a laminated magnetic core. This kind of motor was applied in Maytag Neptune washing machines offered in the USA market. Such a motor is supplied by the American supply system with

120 V voltage and 60 Hz frequency. The static behaviour of that commercially available Emerson Electric motor was previously simulated, measured and analysed [11]. Magnetic flux densities, inductances and electromagnetic torque profiles, as well as flux linkages, were obtained.

Recently, this motor's windings were modified so that the motor could be powered from a converter supplied from the Polish electrical system with a voltage of 230 V. That was a reason to change a configuration of coils in windings from parallel to serial. The magnetic core and number of phases were left unchanged. Changes of configuration caused an increase in resistance and inductance of motors.

The second one motor's magnetic core was made of SMC materials. This newly designed and manufactured motor has elements of an Emerson Electric motor, such as a shaft, bearings and its end shields. That motor has a stator core made of Somaloy 700 powder and a rotor made of Somaloy 700HR powder. Both SMC powders were produced by Swedish company Höganäs AB. In addition, a new winding was designed for the new motor. Stator and rotor cores were manufactured in Lukasiewicz Research Network – Tele and Radio Research Institute. It was impossible to obtain an entire stator core in one piece and an entire rotor core in one piece, so the cores were assembled from smaller parts connected to each other by glue.

The modified Emerson Electric motor (MEE) and the soft magnetic composite (SMC) motor performance were measured and compared. The MEE motor develops higher torque at low speeds, whereas the SMC motor develops higher torque at higher rotational speed. Maximum available power is similar in those two kinds of motors and is about 220 W. The drive with the motor with a soft magnetic composite core has higher efficiency, about 71%, which is 8% higher than a modified Emerson Electric motor has. Thermal measurements of the motors showed that the maximum temperature of windings of the prototype was equal to 67°C, and was about 10°C lower than in the commercial one. Both motors were loaded with the same torque, $T = 0.35$ Nm, and the same speed, $n = 4400$ rpm [12].

The main aim of the research is to compare static characteristics of the modified commercial switched reluctance motor with the prototype one, such as inductance and electromagnetic torque. Comparison of simulations and measurements were also carried out.

The article is organized in such a way: after the introduction, analyzed motors are presented, then methods and measurement stand for inductance and torque determination. Methods of determining magnetization curves of magnetic materials are also presented. The results of measurements of magnetization curves are shown. Next, inductance and torque are simulated and measured. In the further part of the paper flux linkage and flux densities are simulated and presented. In the last part of the article values of the measured and developed average and maximum torques are compared and discussed. In the end of the article discussion and conclusion are presented.

## 2. Methods of inductance and torque determination

Two kinds of motors were used in the research. The first one was the modified Emerson Electric (MEE) motor and the second one was the prototype with a magnetic core made of SMCs and is called a SMC motor. Figure 1 shows structures of the analyzed motors.

Table 1 shows parameters of the MEE and SMC motors.

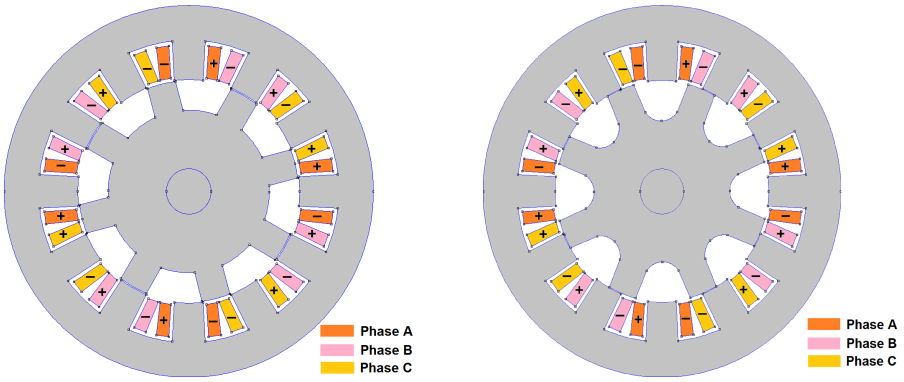


(a) (b)

Fig. 1. Structures of analysed motors: modified Emerson Electric (a); prototype with soft magnetic composite core (b)

Table 1. Parameters of modified Emerson Electric motor and prototype made of soft magnetic composites (SMCs)

| **Parameter** | **Modified Emerson Electric motor** | **Prototype made of SMCs** | **Unit** |
|---|---|---|---|
| DC supply voltage | 310 | 310 | V |
| Max. rotational speed | 9000 | 9800 | rpm |
| External stator diameter | 139.5 | 139.5 | mm |
| External rotor diameter | 83 | 83 | mm |
| Axial length of magnetic core | 47.3 | 46.6 | mm |
| Air gap length | 0.4 | 0.25 | mm |
| Number of phases | 3 | 3 | – |
| Number of stator poles | 12 | 12 | – |
| Number of rotor poles | 8 | 8 | – |
| Material of stator core | Fe-Si laminations | Somaloy 700 | – |
| Material of rotor core | Fe-Si laminations | Somaloy 700HR | – |
| Phase resistance | 8.4 ± 0.3 | 5.7 ± 0.3 | Ω |
| Coil turns | 172 | 134 | – |
| Wire diameter | 0.56 | 0.60 | mm |
| Phase inductance – aligned | 228 | 135 | mH |
| Phase inductance – unaligned | 36 | 24 | mH |
| Stator pole angle | 15.5 | 15.5 | ° |
| Rotor pole angle | 16 | 16 | ° |
| Moment of inertia | 0.00098 | 0.00090 | kg·m$^2$ |

For the proper analyse and simulation of magnetic electric motors, the characteristics of materials used in their construction are needed. Computer simulations are used for the prediction of parameters of motors or the comparison of measurements with calculations. Numerical calculations are also needed for ensuring that measurements of motors are conducted in a proper way and the results are comparable with simulations. The magnetic properties of three materials used in the construction of motors were measured. The first one was electrical steel sheet taken and cut from an Emerson Electric motor, the second one was Somaloy 700 composite material, and the third one was Somaloy 700HR with higher resistivity than Somaloy 700 that were used as stator and rotor cores of the prototype motor. Measurements of magnetization characteristics $B = f(H)$ for DC and AC – 50 Hz conditions were conducted. DC characteristics were used for torque simulations, whereas AC characteristics were for inductance measurements. Magnetization characteristics were measured on toroidal samples with the usage of a hysteresisgraph made by Laboratorio Elettrofisico Engineering company according to IEC standards. DC magnetization characteristics were measured according to IEC 60404-4, whereas AC characteristics were measured according to IEC 60404-6 standards.

Electromagnetic simulations using the finite element method (FEM) were conducted with the use of two-dimensional FEMM 4.2 software [13]. For these two motors, the comparison of simulations and measurements of inductances as a function of a position between stator and rotor cores was conducted. The comparison of developed torques as a function of rotation angles and currents was also conducted.

Inductance measurements were conducted on the measuring stand shown in Fig. 2. The method of inductance determination is based on the calculation of impedance from voltage and current measurements made at a frequency of 50 Hz. The inductance calculation takes into consideration the phase resistance.

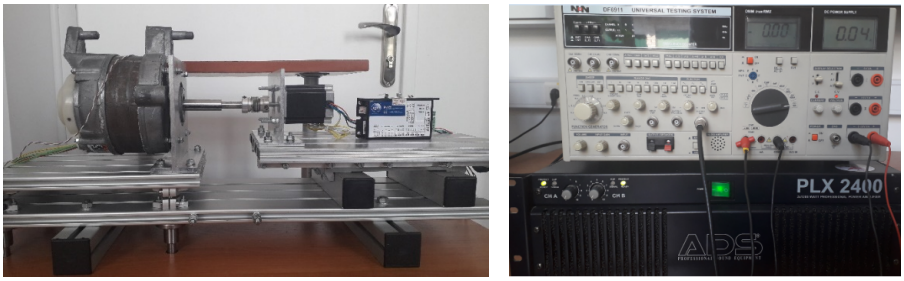


(a) (b)

Fig. 2. Measuring stand (a) and devices for inductance determination (b)

The measuring stand contains the measured motor connected with a two-phase stepper motor 57BYGH803 with a SIC 174 controller made of Wobit that is used for changes of angles between stators and rotors. A sinusoidal function generator and power amplifier were used for energizing motor windings. The function generator is a part of the Universal Testing System model DF6911 made by the NDN company, whereas the power amplifier was made by the ADS company, model PLX 2400 with a power of 1200 W. Phase currents were measured with an RMS ammeter that

is also a part of Universal Testing System. Voltages and their frequencies were measured with a Fluke 115 multimeter.

Electromagnetic torque was measured on the stand shown in Fig. 3. It uses the same stepper motor as in the inductance measurements, whereas torque was measured with a torque meter MW2006-3S, and sensor MT-3Nm manufactured by Roman Pomianowski Electronics Lab.

Fig. 3. Measuring stand for torque measurements

## 3. Determination of magnetization curves, inductance and torque of composite and laminated motors

### 3.1. Measurements of magnetization characteristics of laminated and composite materials

Figure 4(a) shows a comparison of DC characteristics for steel sheets and composites, whereas Fig. 4(b) for AC characteristics.

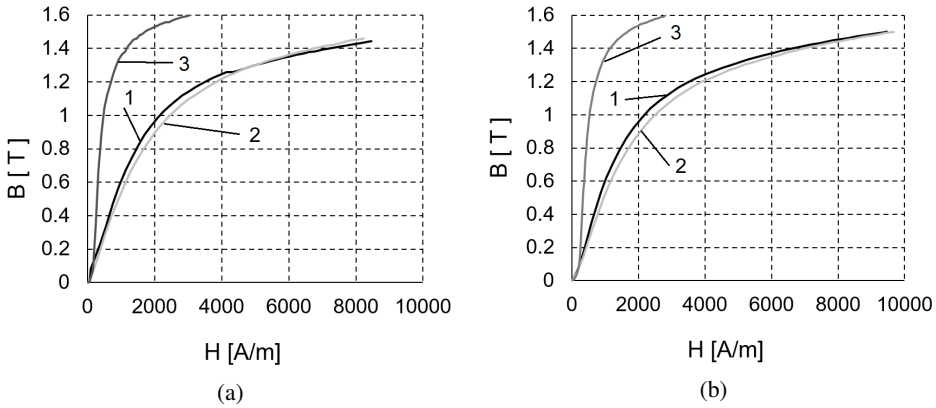


Fig. 4. Magnetization characteristics for materials used in motors, 1 – Somaloy 700, 2 – Somaloy 700HR, 3 – electrical steel: DC (a); AC – 50 Hz (b)

As it can be seen from Fig. 4(a), the characteristics are nonlinear and electrical steel has the highest permeability (the highest magnetic flux density $B$ at the same magnetic field strength $H$) – curve 3, whereas for Somaloy 700HR the lowest – curve 2. The same situation is for the AC magnetization curves.

Figure 5(a) shows a comparison of AC and DC magnetization curves for Somaloy 700 composite, Fig. 5(b) for Somaloy 700HR, and Fig. 6 for electrical steel sheets.

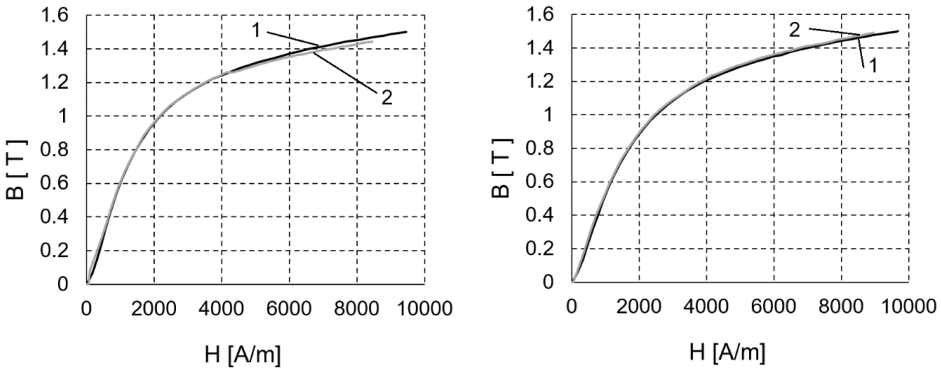


Fig. 5. Magnetization curves for Somaloy 700 (a), Somaloy 700HR (b): 1 – AC-50 Hz, 2 – DC

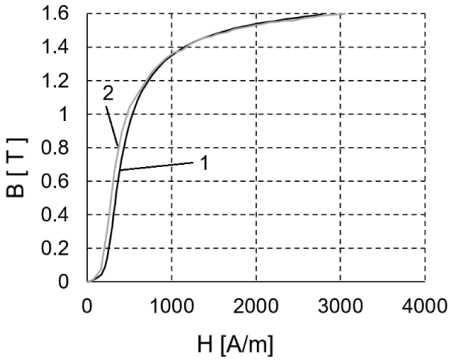


Fig. 6. Magnetization curves for electrical steel: 1 – AC 50 Hz, 2 – DC

The magnetization characteristics for AC with 50 Hz and DC for Somaloy 700 and Somaloy 700HR are almost the same (Fig. 5(a) and 5(b)). It can be seen in Fig. 6 that the curves of electrical steel for the magnetic field strength H from 0 to 700 A/m differ a lot, above 700 A/m are almost the same. The maximum difference of magnetic permeability for AC 50 Hz and DC condition is for 300 A/m. Magnetic permeability for AC condition $\mu$ = 1 000, whereas for DC condition $\mu$ = 1600.

Overall, different behaviour of magnetic materials under DC and AC conditions influence parameters of electric motors. Somaloy magnetic materials have the same magnetization curves, whereas electrical steel sheets are different at DC and AC supply. It is due to different resistivity of materials and eddy currents induced by changing magnetic flux. Eddy currents decrease effective permeability and cause an increase in coercivity which causes, in effect, higher iron loss. The Somaloy 700 material has, according to manufacturer's data, a resistivity of $\rho$ = 400 μΩm,

Somaloy 700HR a resistivity of $\rho = 1000$ μΩm. In turn, oriented electrical steel's resistivity for electric motors depends on the amount of silicon in an alloy, but for typical oriented steel, resistivity is $\rho = 0.54$ μΩm. Changes in magnetization curves between DC and AC conditions will be more visible if the frequency of magnetic flux density will be higher than 50 Hz. The magnitude of differences in the resistivity between powder composite and Fe-Si laminations are great, about 1000 to 2000 times. Such a difference will have an influence on the iron loss in a rotating motor, especially while working at a high speed of 9 000 rpm for MEE, and a high speed of 9800 rpm for SMC motors when magnetic flux frequency can be as high as about 1200 Hz for MEE and 1300 Hz for SMC motors. These high frequencies of magnetic flux occur in the stator's poles and yoke causing power loss where windings are placed and the danger of their damage by high temperature.

### 3.2. Simulations of magnetic flux densities in motors

The distribution of magnetic flux density in motors was calculated for the same current linkage, for aligned poles and for an angle of 15° between the stator and rotor poles. The magnetic flux density distribution in motors was obtained from FEM calculations using the FEMM 4.2 software. During the calculations, the simulation region was discretized into approximately 100 000 elements with 50 000 nodes.

Figure 7(a) shows the magnetic flux density in the MEE motor, Fig. 7(b) in the SMC motor for aligned poles, Fig. 8(a) for an angle of 15° between the stator and rotor poles in the MEE motor, and Fig. 8(b) for the same angle for the SMC motor. An angle of 15° is the angle with maximum torques.

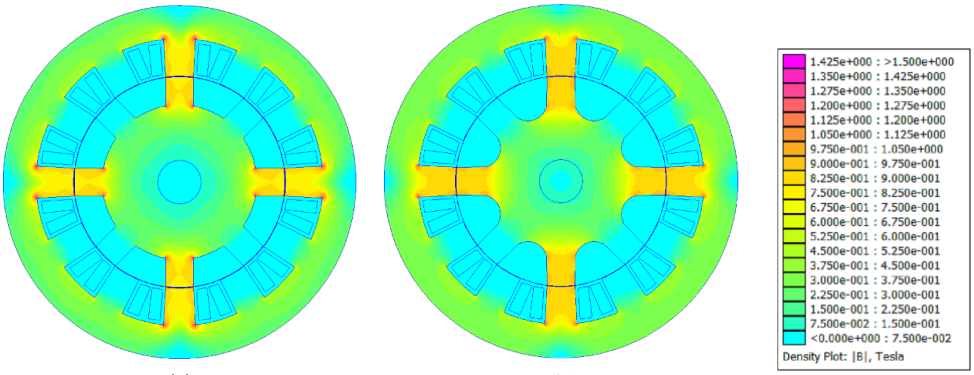


(a) (b)

Fig. 7. Distribution of magnetic flux density for: the modified Emerson Electric motor, $I = 1.6$ A, $B_{max} = 1.4$ T (a); the prototype motor, $I = 2$ A, $B_{max} = 1.5$ T (b), for aligned poles

For the aligned poles in the modified Emerson Electric motor, the magnetic flux density for the stator and rotor poles is $B = 0.8$ T, for the stator core, $B = 0.35$ T, whereas for the rotor core, $B = 0.25$ T. For the aligned poles in the prototype motor, the magnetic flux density for the stator and rotor poles is $B = 0.9$ T, for the stator core, $B = 0.4$ T, and for the rotor core, $B = 0.3$ T.

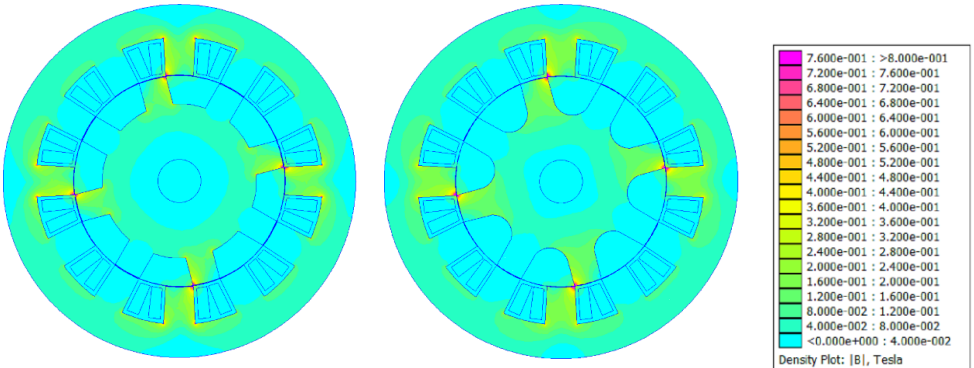


(a) (b)

Fig. 8. Distribution of magnetic flux density for: the modified Emerson Electric motor, $I$ = 1.6 A, $B_{\max}$ = 0.8 T (a); the prototype motor, $I$ = 2 A, $B_{\max}$ = 0.9 T (b), for 15° between poles

When the angle between stator and rotor poles in the MEE and SMC motors is equal to 15°, the observed magnetic flux density for the stator and rotor poles is equal to $B$ = 0.2 T, for the stator core, $B$ = 0.1 T, and for the rotor core, $B$ = 0.7 T. Almost the same magnetic flux density can be observed for nearest pole edges, for both motors, here $B$ = 0.8 − 0.9 T.

### 3.3. Simulations and measurements of motors inductance and flux linkages

The results of inductance simulations and measurements are shown in Fig. 9. Figure 9(a) presents the measured and simulated inductance of the MEE motor, whereas Fig. 9(b) shows the measured and simulated inductance of the SMC motor. The measurements of the MEE motor were done with sinusoidal currents $I_{RMS}$ = 0.5 A, whereas of the SMC motor with sinusoidal currents, $I_{RMS}$ = 0.65 A at 50 Hz. These currents ensure the same current linkage for those two motors. The simulations of inductance were conducted taking into account the amplitude magnetization curves $B_m = f(H_m)$ of steel laminations and composites. The simulations for an Emerson Electric motor were executed at the amplitude of currents equal to $I_m$ = 0.7 A and for the SMC motor, $I_m$ = 0.9 A. These currents ensure the same supply conditions.

As it can be seen from Fig. 9, the measured values of inductances for both motors are higher than those simulated. It is due to the 2D simulation model neglecting the end windings and the effects associated with them. According to literature, a 2D model can have lower inductance by about a few percent in the aligned position in comparison to measurements and by 20–30% in the unaligned position [14]. Since the inductances were measured with changing magnetic flux density and field strength, whereas the simulations for static conditions, this situation also influences the values of inductances. It is caused by neglecting eddy currents in steel sheets. In the measurements, eddy currents caused a decrease in permeability and inductances. In the case of magnetic composites, this phenomenon is not so clearly observed because composites have high resistivity and eddy currents are very small. The decrease between the measured and simulated inductances for the MEE motor for the aligned position is by 23%, and for the unaligned position

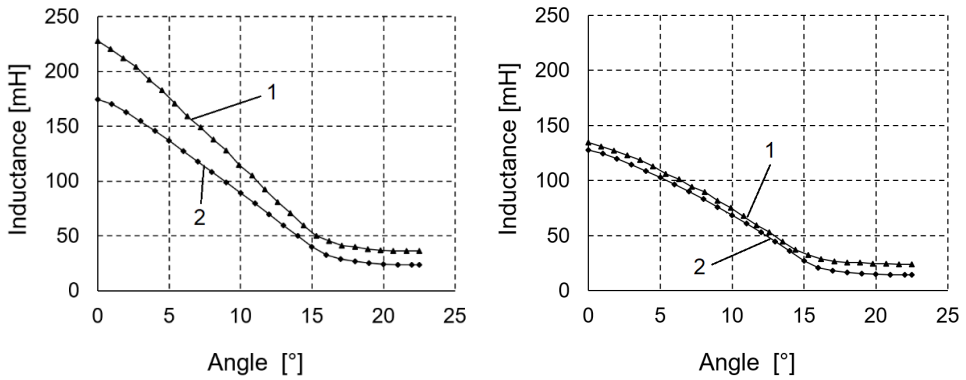


Fig. 9. Measured (1) and simulated (2) inductance of: the modified Emerson Electric motor (a); the prototype motor with SMCs (b); vs angle between stator and rotor poles

by 35%. In turn, the decrease between the measured and simulated inductances for the SMC motor for the aligned position is by 5%, and for the unaligned position by 40%.

Phase flux linkages for the modified Emerson Electric prototype were also calculated. Curves for the aligned and the unaligned positions were determined. Figure 10(a) shows flux linkages for the MEE motor, whereas Fig. 10(b) shows those linkages for the SMC motor.

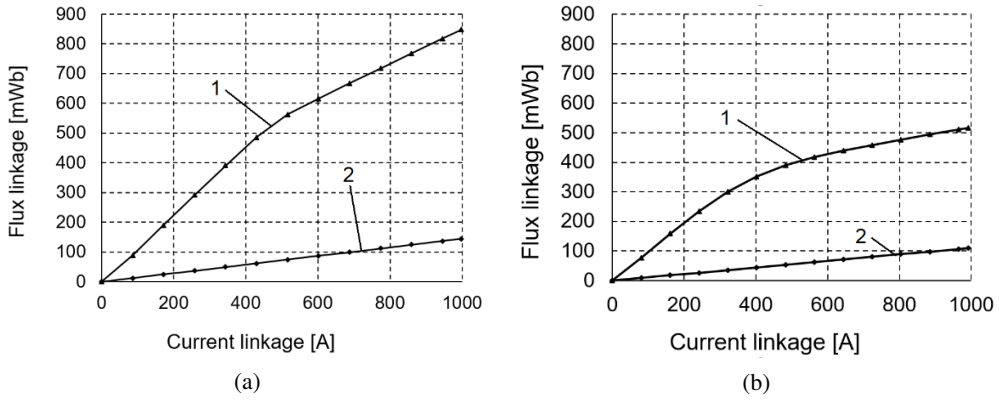


Fig. 10. Flux linkage vs current linkage of 1-aligned position, 2-unaligned position for: modified Emerson Electric motor (a); prototype motor (b)

As it can be seen from Fig. 10, in the case of the same current linkages, the prototype motor has lower flux linkages than the MEE motor. Little saturation can also be observed for current linkages above 450 A for the MEE motor, and 300 A for the SMC motor.

### 3.4. Simulations and measurements of static torque developed by motors

Simulations and measurements of the electromagnetic torque developed by the two motors were conducted and compared. A comparison of the developed torque vs the angle between stator and rotor poles is shown in Fig. 11 for the MEE motor, whereas in Fig. 12 for the SMC motor.

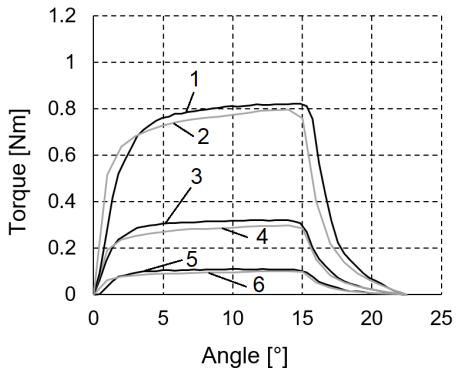


Fig. 11. Electromagnetic torque vs angle between stator and rotor poles, for modified Emerson motor 1 – measured $I$ = 1.6 A, 2 – simulated $I$ = 1.6 A, 3 – measured $I$ = 1 A, 4 – simulated $I$ = 1 A, 5 measured $I$ = 0.6 A, 6 – simulated $I$ = 0.6 A

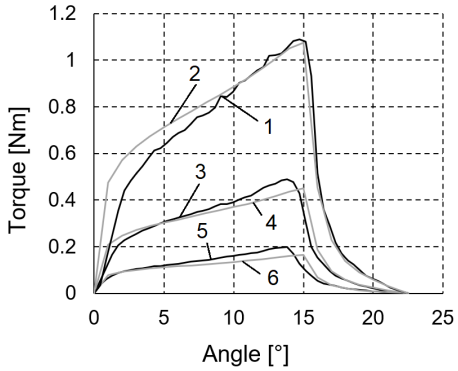


Fig. 12. Electromagnetic torque vs angle between stator and rotor poles, for a prototype motor 1 – measured $I$ = 2 A, 2 – simulated $I$ = 2 A, 3 – measured $I$ = 1.3 A, 4 – simulated $I$ = 1.3 A, 5 measured $I$ = 0.8 A, 6 – simulated $I$ = 0.8 A

Average torque was calculated from the integration of the area under the curve of torque vs angle characteristics for 0° to 22.5° (Fig. 11 and Fig. 12). The same calculation of torque was done for the curves obtained from the measurements for the same conditions, as in calculations.

During rotation, working motors have their turn-on and turn-off angles chosen so that each phase generates the maximum torque, which is a conduction angle of about 15°. After such degrees of rotation, the first phase stops conducting current, whereas the second phase starts its conducting. After the next period of the conduction, the third phase is energized and then the first phase starts to conducts current.

The electromagnetic energy that is available to be converted into mechanical work can be calculated from the flux linkage curves for the aligned and unaligned rotor and stator poles. The average torque $T_{\text{avg}}$ has been calculated according to Formula (1) from the area between the aligned and unaligned curves for the defined current (see Fig. 10) [14]:

$$T_{\text{avg}} = \frac{SW}{2\pi} = \frac{mN_r W}{2\pi}, \tag{1}$$

where: $S$ is the number of strokes per revolution $S = 24$, $m$ is the number of phases $m = 3$, $N_r$ is the number of rotor poles $N_r = 8$, $W$ defines the maximum energy converted from electrical to mechanical.

Maximum energy converted from electrical to mechanical $W$ can be calculated for linear changes of flux linkage with current, practically as an area of a triangle, limited by curves of the aligned, unaligned flux linkages, and value of current:

$$W = 0.5\,(\Psi_a - \Psi_u)\,I, \tag{2}$$

where: $\Psi_a$ is the flux linkage for the aligned position, $\Psi_u$ is the flux linkage for the unaligned position, and $I$ is the current for calculation.

Table 2 shows the measured and calculated torques developed by motors. For comparison purposes, torques were calculated and measured for the same current linkages. A phase current of 0.6 A for the modified Emerson motor gives the same current linkage of 0.8 A for the prototype one. The same is for current 1 A (modified Emerson) and 1.3 A (prototype) and for 1.6 A (modified Emerson) and 2 A (prototype).

Table 2. Measured and calculated torques of developed motors

| **Kind of motor** | **Phase current $I_{DC}$** | **Current linkage** | **Maximum torque measured** | **Maximum torque calculated** | **Average torque measured** | **Average torque calculated** | **Available average torque calculated from eq. (1)** |
|---|---|---|---|---|---|---|---|
| | [A] | [A] | [Nm] | [Nm] | [Nm] | [Nm] | [Nm] |
| Modified Emerson | 0.6 | 103 | 0.11 | 0.10 | 0.07 | 0.07 | 0.11 |
| | 1 | 172 | 0.32 | 0.30 | 0.20 | 0.22 | 0.32 |
| | 1.6 | 275 | 0.82 | 0.80 | 0.53 | 0.55 | 0.83 |
| Prototype | 0.8 | 107 | 0.20 | 0.17 | 0.09 | 0.10 | 0.14 |
| | 1.3 | 174 | 0.49 | 0.45 | 0.25 | 0.25 | 0.38 |
| | 2 | 268 | 1.09 | 1.08 | 0.59 | 0.55 | 0.87 |

As it can be seen from Table 2, the maximum and average torques for the SMC motor are higher than for the MEE motor with practically the same current linkages. The prototype motor has higher maximal torque than the Emerson one – from 33% to 82%, and from 0% to 43% for the average torque. It is due to smaller air-gap thickness in the prototype motor. Since Fe-Si laminations used in the modified Emerson motor have better magnetizability in comparison to the composite magnetic core, the difference between the torques in the prototype and Emerson motors decreases. The measured and calculated torques are quite close, the maximum percentage deviation of the calculated values from the measured one for the modified Emerson Electric motor is equal to 10%, whereas for the prototype motor it is 15%. Moreover, the available average calculated torque is larger in comparison to the measured and calculated average torques.

The values of maximum electromagnetic torques for different currents were measured and calculated based on FEM simulations. Figure 13(a) shows characteristics for the MEE motor, whereas Fig. 13(b) for the SMC motor.

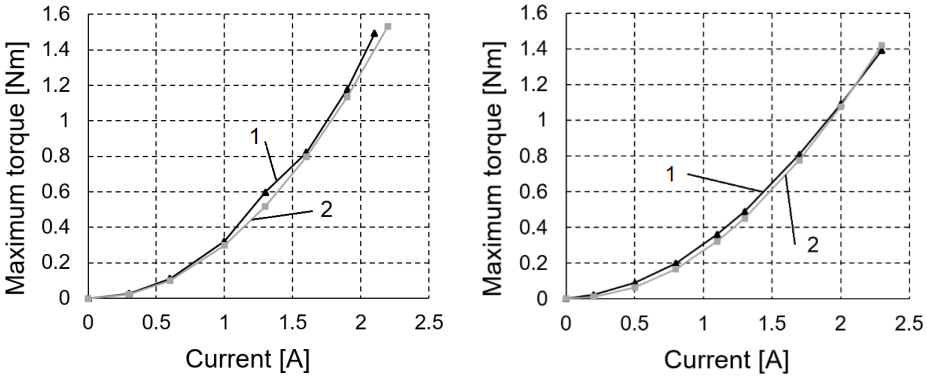


Fig. 13. Characteristics of torque vs current for: the modified Emerson Electric motor (a); the prototype motor (b), 1 – measurements, 2 – calculations

As it can be seen from Fig. 13, the curves shown for the calculated and measured torques are quite close in terms of values and shapes. The maximum torque resembles a parabola and rises with the currents in the second power.

## 4. Summary and discussion

In the first part of the research, the magnetization curves of materials used to construct motors were compared. The comparisons were conducted for a DC and AC of 50 Hz. Three types of materials were analysed, such as Fe-Si steel, Somaloy 700 and Somaloy 700HR composite materials. Fe-Si steel has better magnetizability in comparison to powder materials. However, the comparison of the materials at a DC and AC of 50 Hz shows that the steel material exhibits a decrease in magnetic permeability, whereas the powder materials have almost the same permeability.

The comparison of two SRMs was conducted on the basis of simulation carried out in the FEM software and measurements. Two types of motors under investigation have shown similar performancein terms of the developed torques. The prototype motor has higher maximum, and average torques in comparison to the modified Emerson Electric motor for the same current linkages.

The measurements and simulations of the motors' properties will be useful in further analyses of switched reluctance motors, especially with their efficiency and analysis of power losses.

**References**

[1] Miller T.J.E., *Brushless permanent-magnet and reluctance motor drives*, Oxford University Press (1989).

[2] Krishnan R., *Switched reluctance motor drives: modelling, simulation, analysis, design, and applications*, CRC Press (2001).

[3] Ahn J.-W., *Switched reluctance motor*, in book Torque control Ed. Lamchich M.T., Intech (2011), DOI: 10.5772/10520.

[4] Lawrenson P.J., Stephenson J.M., Blenkinsop P.T., Corda J., Fulton N.N., *Variable-speed switched reluctance motors*, IEE Proceedings B. (Electric Power Applications), vol. 127, no. 4, pp. 253–265 (1980), DOI: 10.1049/ip-b.1980.0034.

[5] Widmer J.D., Martin R., Kimiabeigi M., *Electric vehicle traction motors without rare earth magnets*, Sustainable Materials and Technologies, vol. 3, pp. 7–13 (2015), DOI: 10.1016/j.susmat.2015.02.001.

[6] Riba J.-R., López-Torres C., Romeral L., Garcia A., *Rare-earth-free propulsion motors for electric vehicles: A technology review*, Renewable and Sustainable Energy Reviews, vol. 57, pp. 367–379 (2016), DOI: 10.1016/j.rser.2015.12.121.

[7] Nakamura H., *The current and future status of rare earth permanent magnets*, Scripta Materialia, vol. 154, pp. 273–276 (2018), DOI: 10.1016/j.scriptamat.2017.11.010.

[8] Coey J.M.D., *Magnetism and Magnetic Materials*, Cambridge University Press (2010).

[9] Shokrollahi H., Janghorban K., *Soft magnetic composite materials (SMCs)*, Journal of Materials Processing Technology, vol. 189, no. 1–3, pp. 1–12 (2007), DOI: 10.1016/j.jmatprotec.2007.02.034.

[10] Périgo E.A., Weidenfeller B., Kollár P., Füzer J., *Past, present, and future of soft magnetic composites*, Applied Physics Reviews, vol. 5, no. 3 (2018), DOI: 10.1063/1.5027045.

[11] Przybylski M., *Modelling and analysis of the low-power 3-phase switched reluctance motor*, Archives of Electrical Engineering, vol. 68, no. 2, pp. 443–454 (2019), DOI: 10.24425/aee.2019.128279.

[12] Przybylski M., Ślusarek B., Di Barba P., Mognaschi M.E., Wiak S., *Temperature and torque measurements of switched reluctance actuator with composite or laminated magnetic cores*, Sensors, vol. 20, no. 3065, pp. 1–14 (2020), DOI: 10.3390/s20113065.

[13] Meeker D., *Finite element method magnetics – User's manual*, ver. 4.2 (2018).

[14] Miller T.J.E., *Optimal design of switched reluctance motors*, IEEE Transactions on Industrial Electronics, vol. 49, no. 1, pp. 15–27 (2002), DOI: 10.1109/41.982244.